CrossMark

Seismic microzoning of Arica and Iquique, Chile

Alix Becerra[1] · Luis Podestá[1] · Roberto Monetta[4] ·
Esteban Sáez[1,2] · Felipe Leyton[3] · Gonzalo Yañez[1,2]

Abstract This paper focuses on a geophysical-based analysis of the soils in Arica and Iquique, both main cities in northern Chile. The large seismogenic coupling and the 136-year seismic gap predispose the north of the country to the highly likely seismic activity that could affect this area. This seismotectonic scenario highlights the importance of the assessment of earthquake hazards in urban domains. In this context, seismic microzoning emerges as a tool to identify areas that are more or less susceptible to ground motion amplification. In both cities, 148 sites were chosen to perform geophysical surveys based on surface wave methods, namely the spatial autocorrelation, frequency-wave number and H/V spectral ratio techniques. By inverting the measurements, local shear wave velocity profiles and predominant frequencies were derived. Additionally, seven boreholes were drilled to further complement the gathered data. With the available results, the cities were

✉ Esteban Sáez
  esaez@ing.puc.cl

  Alix Becerra
  aabecerr@ing.puc.cl

  Luis Podestá
  l.podesta@dictuc.cl

  Roberto Monetta
  roberto.monetta@gmail.com

  Felipe Leyton
  felipe@dgf.uchile.cl

  Gonzalo Yañez
  gyanez@ing.puc.cl

[1] School of Engineering, Pontificia Universidad Católica de Chile, Av. Vicuna Mackenna 4860, Macul, Santiago, Chile

[2] National Research Center for Integrated Natural Disaster Management CONICYT/FONDAP/15110017, Av. Vicuna Mackenna 4860, Macul, Santiago, Chile

[3] Centro Sismologico Nacional, Blanco Encalada 2002, Santiago, Chile

[4] School of Engineering, Universidad Diego Portales, Av Ejercito 441, Santiago, Chile

subdivided into different zones with similar properties in terms of the average shear wave velocity on the upper 30 m (V_S^{30}) and the predominant site's frequency F_0; these were parameters that were found consistent with the geology of each city. The collected information suggests zones that are more prone to ground motion amplification, namely: the northern side of Arica, the south-east area of Iquique, the northern limit of Iquique and the artificial landfill of the port of Iquique. The microzoning was compared to the ground motion records of the April 1, 2014, Iquique earthquake and showed to be consistent with the expected motion amplification in Iquique.

1 Introduction

The subduction of the Nazca plate beneath the South American plate places Chile as a country facing major seismic activity. The north of the country had not experienced any large earthquakes in the past 136 years (Fig. 1) until April 1, 2014 (A01-2014), where a major event of 8.2 Mw with a rupture length of about 200 km occurred near the city of Iquique. The estimated recurrence interval of 111 ± 33 years (Comte and Pardo 1991) and the highly coupled rupture zone (Chlieh et al. 2011) (Fig. 1) suggested that such a major event would be imminent. However, despite this prediction, the seismic energy released
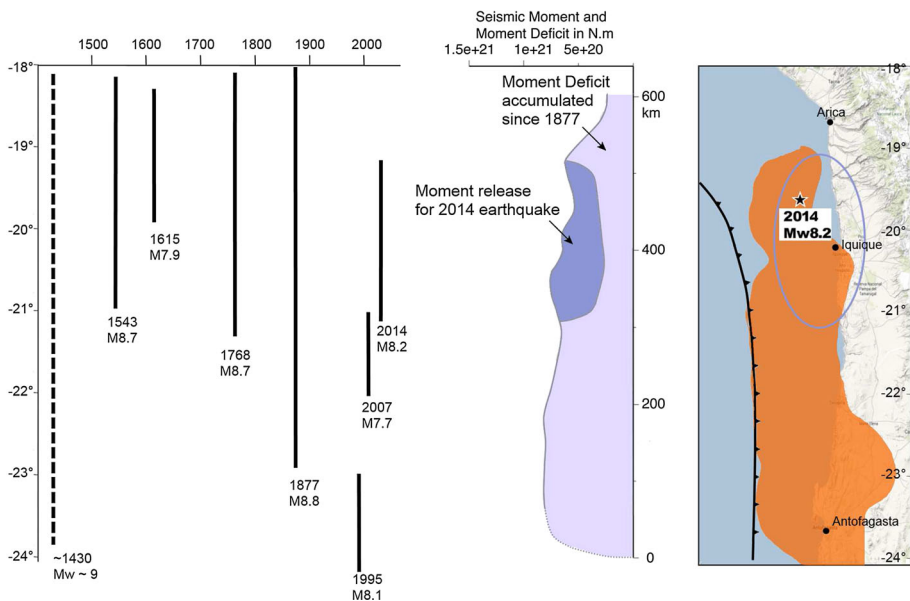

Fig. 1 Seismic context of Northern Chile. To the *left*, the seismic history shows the seismic gap of 136 years that had affected this zone from 1877 to 2014. The image to the *right* shows the interseismic coupling of over 75 % in the area in *orange* and a comparison between the moment deficit accumulated since 1877 and the seismic moment released for the April 1, 2014, event. The rupture area of the earthquake is marked in a *blue line*, obtained from the USGS Earthquake Data Report. Modified from Scholz and Campos (2012) and Chlieh et al. (2011)

during this earthquake was only about 1/6 of the expected energy accumulated (Fig. 1); hence, the moment deficit accumulated remains large (Chlieh et al. 2011) and other events are likely to occur in the near future, presumably to the north and south of the A01-2014 rupture zone. Therefore, actions to prevent human and infrastructure losses in this part of the country are still mandatory. Following this rationale, several studies were conducted in the north of Chile prior to the A01-2014 event (FONDEF Project D10I1027). Among the different strategies followed, seismic microzoning was selected as a tool to assess the earthquake hazards and for predicting site amplification susceptibility within a city.

It is well known that one of the factors that contributes most to damages in urban areas is the proximity to the hypocenter. Nonetheless, soil amplification effects can be crucial during an earthquake due to local geology (Chavez-Garcia et al. 2005). To anticipate this effect, seismic microzoning can provide reliable information about the soil conditions in specific areas within a city that may be prone to site effects. In this research, seismic microzoning was carried out through geophysical surveys based on surface wave methods (SWM). This has been applied in many cities and proven to be reliable to assess site effects (Chavez-Garcia and Cuenca 1998; Scott et al. 2006; Tuladhar et al. 2004), it is also advantageous because of their low-cost, noninvasive effects and versatility.

In the following research, a qualitative seismic microzoning was performed in two main cities of Northern Chile, specifically Arica and Iquique. In the first section, the geological settings will be described to contextualize the problem. Then, a description of the surveys, the selection of sites and the surveys performed in each city will be detailed. In every site, a shear wave velocity profile and a predominant frequency (F_0) are derived from different methods using surface wave records. The shear wave velocity profile will be summarized in terms of its average on the upper 30 m, V_S^{30}, a parameter that is widely used to seismic site classification; this will be combined with F_0 and the boreholes drilled in each city to delimitate areas with similar characteristics that may indicate the susceptibility to ground motion amplification. Finally, we use the recorded ground motions of the A01-2014 earthquake in Iquique to compare the observed and expected site amplification, to evaluate the consistency of the scientific rationale that was adopted.

2 Geological setting

Arica and Iquique are two cities located in the coastal plain of Chile, enclosed to the west by the Chilean Coastal Range, which ends in the southern urban limit of Arica, at El Morro hill. Together they account for over 400.000 inhabitants, 79 % of the population of the northern region, making them the major urban areas in the north of Chile.

2.1 Arica

The city of Arica is located on a sedimentary basin that extends from El Morro hill to the Lluta's alluvial fan. The basement is composed of Jurassic and Paleogene formations of volcano-sedimentary rocks (García et al. 2004). Figure 2a displays the main lithological units in the city, composted mainly of Quaternary and Neogene deposits. Although seven are described in the literature (Maldonado 2014), they can be grouped into three deposit types that shape the morphology of the city; the south, the area around the river and the northern zone. The south of Arica is characterized by the debris of El Morro and La Cruz hills, with a section of limestone deposits, followed by the alluvial fan of the San Jose's
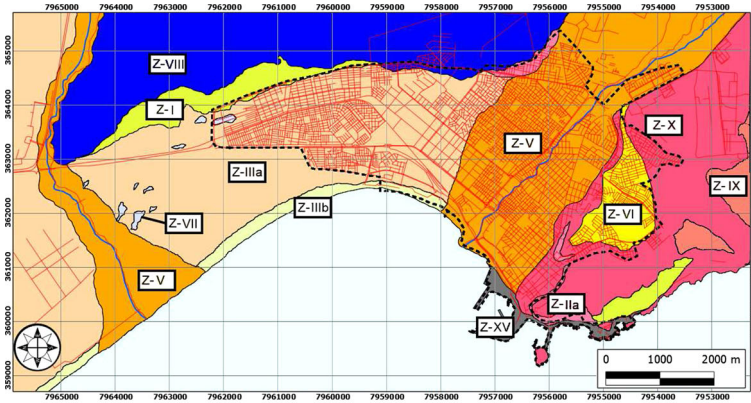
(a) Arica
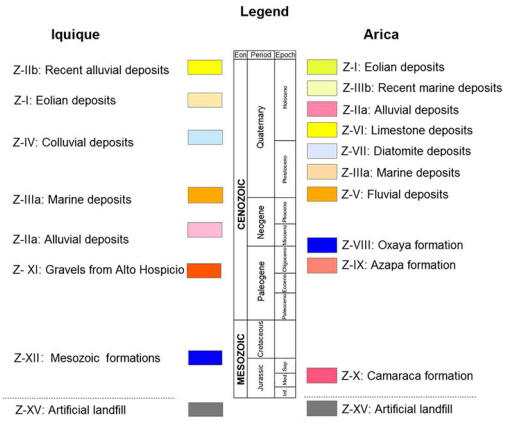
(b) Legend
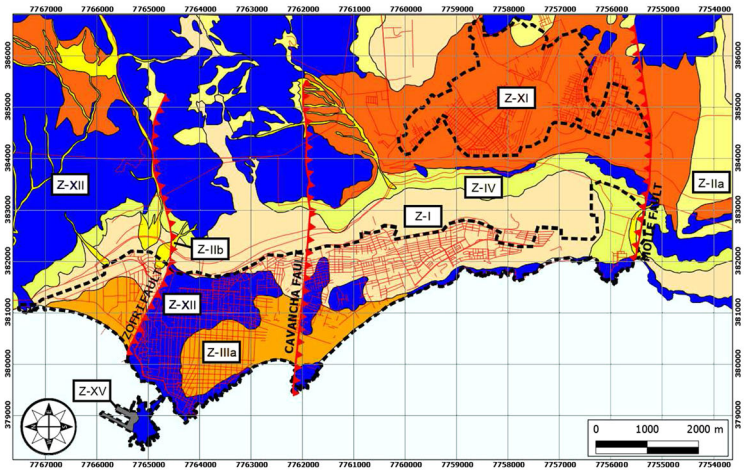
(c) Iquique

river. To the north-east, there can be found a mixture of the debris from El Chuño hill and the deposits from the river. Toward the north, there is an accumulation of eolian sands and marine deposits, with some isolated diatomite deposits in the northern limit of the urban region. The topography is fairly regular inside the city, except for the hills surrounding the basin that rise up to 140 m above sea level.

2.2 Iquique

Unlike Arica, Iquique's geology is very heterogeneous. The city of Iquique comprehends the urban areas of Alto Hospicio and Iquique; both of them are located within the Atacama fault system. Therefore Iquique is a zone crossed by several faults. The main ones that cut the urban area are the ZOFRI Fault, Cavancha Fault and Molle Fault, which can be seen in Fig. 2c. Most of the faults have a predominant E-W strike and a dip of about 60°S, except for the Molle Fault, with a dip of 30°N (Marquardt et al. 2008).

Iquique's surface geology is characterized by the presence of Cenozoic sediments overlying a medium-to-upper Jurassic igneous basement, composed of intrusive and pyroclastic rocks. North from the ZOFRI Fault (Fig. 2c), a 5-m-thick layer of marine deposits can be found (Marquardt et al. 2008). Toward the town center, there is mainly surface bedrock mixed with a random distribution of thin layers of recent marine deposits; furthermore, the Cavancha Fault trace shows a clear separation between the different units. In the south of the city, it is possible to identify the predominance of eolian sediments mixed with debris from El Dragon Hill. Toward the southern urban limit and near the Molle Fault, marine sediments prevail.

Alto Hospicio is located to the south-east of Iquique, about 550 m above sea level over the great escarpment limiting the Coastal Range. The town's geology is characterized by consolidated gravels with a halite matrix (commonly known as rock salt) (Marquardt et al. 2008). Several structural discontinuities in the city have been mapped but have not been properly defined, except for El Molle Fault, that extends inland from the coast.

3 Geophysical survey

The geophysical survey was designed to properly characterize the observed geological units of each city. First, we use available satellite images to select sites that would offer enough space to perform geophysical tests. In each city, we selected 70 sites that met the requirements to perform geophysical surveys using surface wave methods. Afterward, fieldwork took place in Iquique and Alto Hospicio during December 2012 and Arica during January 2013. The measurement of surface waves provides information about the dispersive properties at each site (Tokimatsu 1997); thus, the relationship between the wavelength and phase velocity of a wave. By solving an inverse problem using these data, we are able to identify a shallow shear wave velocity profile in each location. Furthermore, using triaxial sensors we also identify predominant frequencies of the corresponding sites. For geotechnical purposes, the obtained 1D shear wave velocity profile is a key parameter for evaluating dynamic response characteristics in a site (Tokimatsu 1997). There are
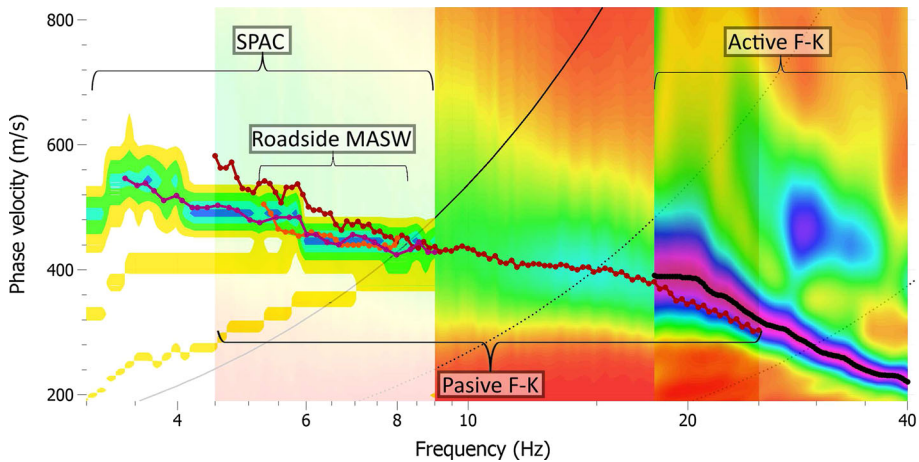
Fig. 3 Extended dispersion curve obtained from the combinations of the techniques: SPAC, active and passive F-K and Roadside MASW. In general terms, a well-defined dispersion curve between 6 and 40 Hz is enough to describe upper 30 m in the explored cities, if lower frequencies are satisfactorily explored, then it is possible to retrieve information in deeper layers. However, the effective explored depth depends on the maximum characterized wavelength that is a function of the minimum frequency and the corresponding phase velocity that varies from one site to another. The *black curved lines* represent the theoretical limits of spatial sampling of the dispersion curve, based on the geometry of the passive F-K array

several methodologies to record and to process the waveforms, depending on the array used to record the data. In this research, we combine source-controlled (active) and ambient noise (passive) techniques based on noninvasive surveys, using vertical sensors deployed in different sets of arrays (Fig. 3). Linear arrays are required for active measurements, and bi-dimensional arrays are suitable for passive methods. Depending on the available space to deploy the arrays, linear arrays were also used for ambient-noise-based techniques. The geometries of the arrays' setup are described in Fig. 4. Active surveys had a sampling rate of 0.125 ms and a recording time of 2 s, whereas for passive sources the recording time was 20 min and a sampling rate of 16 ms.

For these procedures, two types of equipment were used; a Geometrics® Geode-12 seismograph with 12 channels for the circular and linear arrays and a Quanterra® Q330 with 6 channels for the kite-shaped arrays. Vertical sensors were connected to each channel; the devices use geophones with a natural frequency of 4.5 and 1.0 Hz for Geode and Quanterra, respectively.

A methodology has been previously proposed that combines the different techniques to obtain a consistent shear wave profile (Tokimatsu 1997; Humire 2015). The techniques used were:

- F-K: The spectral frequency-wave number method, or simply F-K, is based on the hypothesis that the array is crossed by a plain wave-front, consisting mostly of Rayleigh surface waves (Kvaerna and Ringdahl 1986; Lacoss et al. 1969). It is versatile since it can be used for a passive approach (ambient noise) or an active approach (record of impulsive point source at a known position). 1D and 2D seismic arrays were used for each approach. The registered signals in each geophone are combined, and a time-space Fourier transformation allows analysis of the data in the frequency-wave number domain so an energy spectrum may be constructed according to the recorded
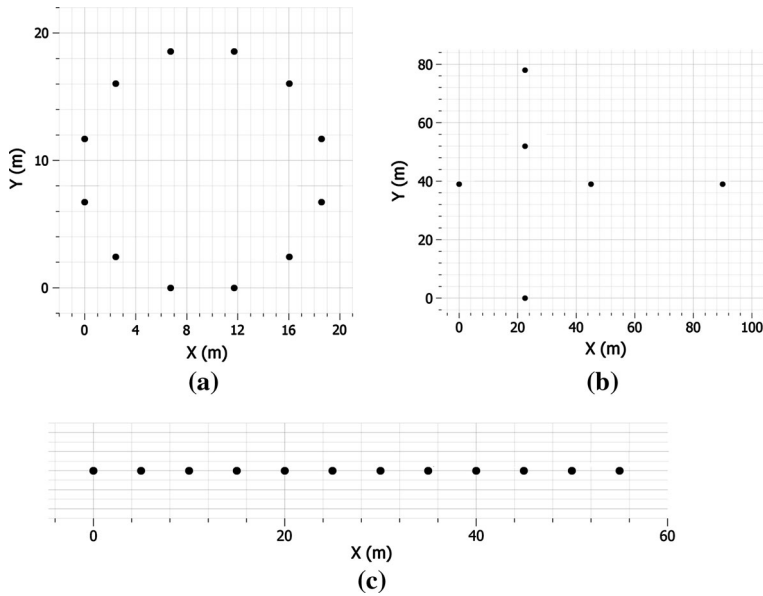
Fig. 4 Types of deployed arrays. Regular linear arrays had a maximum length of 55 m. Bi-dimensional arrays consisted in circles of a maximum radius of about 10 m and kite-shaped arrays with maximum dimensions of 90×78 m. **a** Circular, **b** kite-shaped, **c** linear

waveforms. When the frequency-wave number combination matches with a Rayleigh wave crossing the array, a peak on the F-K spectrum appears, allowing us to identify dispersive properties throughout the dispersion curve. In the case of an active source, an attenuation coefficient is included to take into account the distance of the source to each geophone. Note that for the active approach, a 18-lb sledgehammer was used, doing several surveys at different distances, in order to stack the obtained dispersion curves and thus reduce ambient noise that may negatively affect the procedure.

- SPAC: The spatial autocorrelation method is a technique developed by Aki (1957), on the basis that the wavefield generated by microtremors is a stochastic process, stationary in time and space, and is composed mainly of Rayleigh waves. This principle allows us to predict the spectral energy through the calculation of spatial autocorrelation coefficients between the waveforms of different pairs of geophones located at a certain distance. The use of this methodology requires 2D seismic arrays, although it can also be applied in 1D (linear) arrays (Chávez-García et al. 2006), and it allows us to explore deeper soil layers using exactly the same waveforms. This work has focused on the use of the modified SPAC, proposed by Bettig et al. (2001), that takes into account the autocorrelation between pairs of geophones at different distances.

Additionally, the Roadside MASW methodology was used to further validate the consistency of the dispersion curves. This is a methodology derived from the common active MASW method (Park et al. 1999; Park and Miller 2008). It allows the execution of surveys through a passive approach with linear seismic arrays. It is very convenient for urban areas, where linear arrays could be located on the side of a street. The method usually showed a good match with the other dispersion curves, as depicted in Fig. 3.

Table 1 Used Rayleigh wave methods and performance in this study

Method	Source	Sensor array	Analysis	Applicable depth (m)
Active	Sledgehammer	Linear	F-K analysis	≤15
Passive	Microtremors	Two-dimensional	F-K analysis	10–80
Passive	Microtremors	Linear and two-dimensional	Modified SPAC	20–80
Passive	Microtremors	Linear	Roadside MASW	20–40

Table 1 summarizes the procedures and the applicable depths in this study. Note that with the equipment used, that is, the maximum aperture of arrays and fundamental frequencies of the sensors, we did not explore a V_S profile that would reach bedrock in areas with deep sediments. In a few cases, with the kite-shaped arrays, it was possible to explore as deep as 85 m, but the other surveys did not reach any deeper than 45 m.

Once respective dispersion and autocorrelation curves were obtained, they were superimposed in order to define a dispersion curve that extends in a wide frequency range (2–45 Hz in principle). Figure 3 illustrates a typical result of this combination; generally, a consistent overlap was found between the curves. Afterward, an inversion process was carried out to obtain an adjusted dispersion curve and its corresponding shear wave velocity profile through an improved neighborhood algorithm (Wathelet 2008). This algorithm is a stochastic process that tries to guide the random generation of samples by the results obtained on previous ones, it requires prior information about the geophysical parameters and makes use of Voronoi cells to model the adjustment function. The input for this process is the Poisson ratio, the number of layers, the density, and an estimated range for the body wave velocity and the shear wave velocity of each layer. In this study we used a Poisson ratio and density varying between 0.2–0.4 and 1600–2100 kg/m³ respectively, based on boreholes and geological background, a variable number of layers between 3 and 6, and a body wave velocity profile linked to V_S through the Poisson ratio. The inversion is iterated until reaching a reasonable fit between the adjusted model and the empirical dispersive properties; this is measured through an adjustment value, the misfit, with the following formula (Wathelet et al. 2007),

$$\text{Misfit} = \sqrt{\sum_{i=1}^{n_F} \frac{(x_{r,i} - x_{c,i})}{\sigma_i n_F}} \tag{1}$$

where n_F denotes the total number of sampling frequencies for the dispersion curve, $x_{r,i}$ the value of the phase velocity in that point, σ_i the standard deviation in that point, and $x_{c,i}$ the value of the phase velocity of the adjusted model. The iteration process is repeated until the misfit reaches a minimum value, steady with additional iterations. Generally, we found that a misfit below 0.2 was taken as an acceptable model; however, this may vary and a visual inspection of the adjusted dispersion curve is necessary in order to accept or reject an inversion (Fig. 5).

A difficulty that arises in the inversion problem is when soft layers are trapped between stiff layers. In this case, higher Rayleigh modes must be taken into account when identifying a dispersion curve (Roma and Tononi 2011), and consider inverse stiffness contrasts in the inversion problem. In this study, we did not find sites with inversely dispersive properties, and higher Rayleigh modes were identified in the dispersion graphs in very few cases.
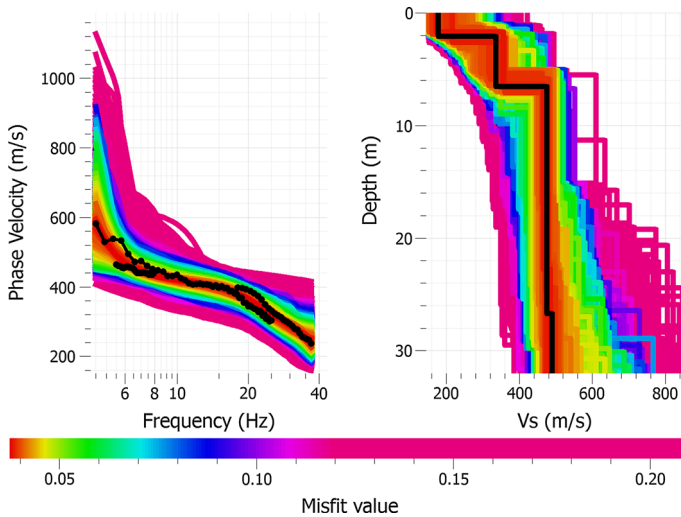
Fig. 5 Inversion process carried out from the experimental data, the figure shows the possible combinations of proposed dispersion curves and shear wave velocity profile, based on the adjustment value for the experimental dispersion curve (misfit). The *black line* indicates the shear wave velocity profile with the minimum misfit selected for the microzoning analysis

A complementary survey carried out in each site was the HV spectral ratio (HVSR) or Nakamura's technique (Nakamura 1989). This method requires one triaxial geophone, and it compares the Fourier spectrum ratio of the horizontal and vertical components of the microtremors registered at the surface. A predominant frequency estimator (F_0) is derived from the identification of peaks in the spectrum. The equipment employed was a Micromed® Tromino three-component data acquisition system. A minimum of three measurements of 20 minutes each were recorded in each site. Typical results of this test are shown in Fig. 6.

Finally, seven boreholes were drilled in both cities in order to verify the reliability and further complement the results of the geophysical surveys. The selection of the sites was based on the geology background that was available at the time of the study. The location of the boreholes and their respective logs are displayed in Figs. 7 and 8. The available borehole samples were used to evaluate the consistency of the geophysical results. Only a classification based on the United Soil Classification System, USCS (Astm 2011), was performed on the samples because most of them were heavily perturbed during their transportation to the laboratories. With the acquired data from the geophysical surveys and boreholes, it is possible to combine and compare the data to properly describe the dynamic characteristics of each site.

4 Results

Seismic microzoning consists of refined seismic zoning data that provides information about the degree of ground motion amplification at different locations within an area. The analysis and interpretation of the geophysical data in Arica and Iquique allowed us to study the dynamic properties of the soil and evaluate their consistency with the surface geology
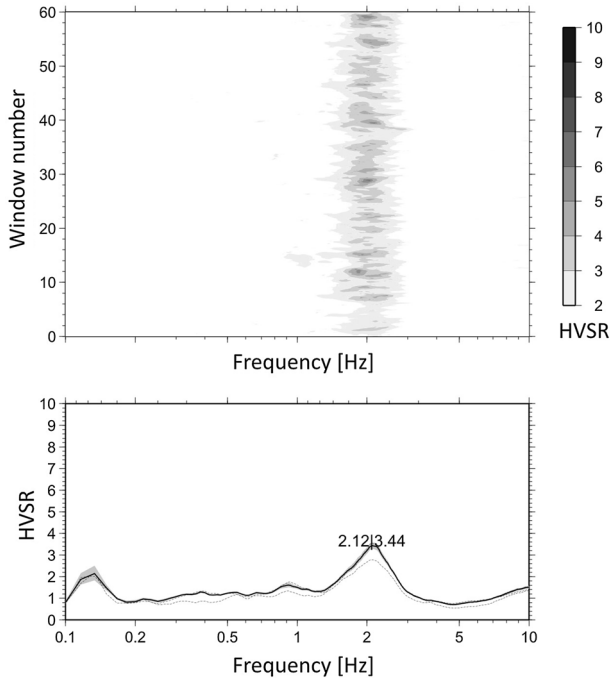
Fig. 6 Example of microtremors' HVSR for one site. The first image (*bottom*) shows the geometrical mean of the spectrum (*continuous line*) and its corresponding standard deviation in log scale (*gray area*). The second image (*top*) indicates the predominant frequency by time window; in other words, it is an indicator of the stability of the result (Leyton et al. 2013). The text located on the peak corresponds to the selected predominant frequency with its corresponding amplitude

and the A01-2014 earthquake response, looking for zones that will be more prone to site effects.

The parameters used to evaluate the dynamic properties of each site are the predominant frequency obtained from the HVSR, F_0, its according amplitude, A_0, the harmonic average of the shear wave velocity for the upper 30 m, V_S^{30}, the borehole logs and the geological background.

The derived results from the geophysical surveys in Arica and Iquique are illustrated in Figs. 9 and 10. In Figs. 9a and 10a the predominant frequency from application of Nakamura's technique is displayed, with a scale relative to the value of F_0 in color, and the value of the amplitude A_0 in size. As shown in the literature (Pilz et al. 2010; Leyton et al. 2013), the value of the amplitude may be a relevant indicator of impedance contrast between the different materials. It is also important to take into account that many HVSR surveys were carried out in each site, but only one result is shown in the map for a better visualization. The selection was based on the best-fitting curve to the SESAME guidelines (Acerra et al. 2004).
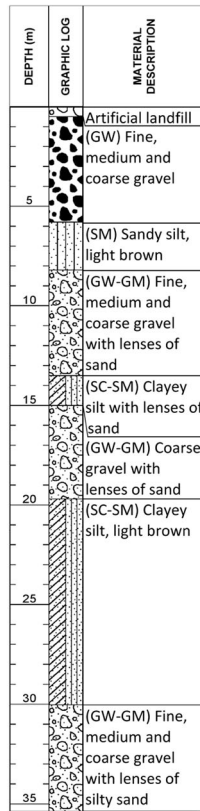
4.1 Arica

The results of the tests in Arica are shown in Fig. 9. They show that the city is characterized by relative low velocities except for the south, on El Morro hill. The high
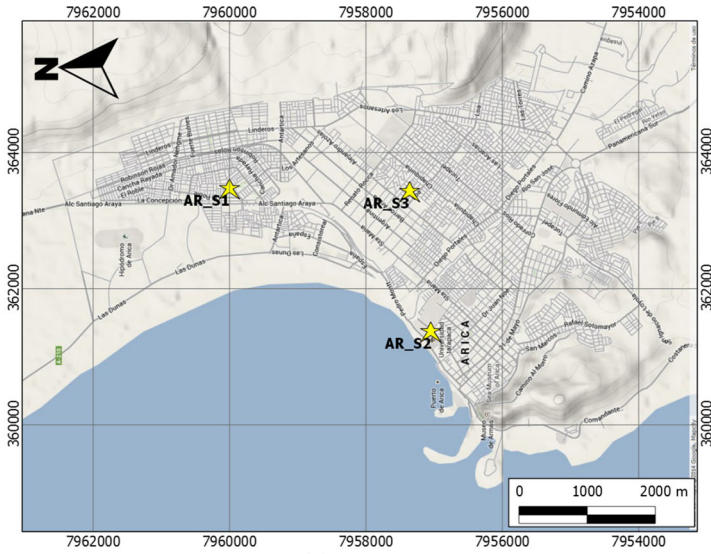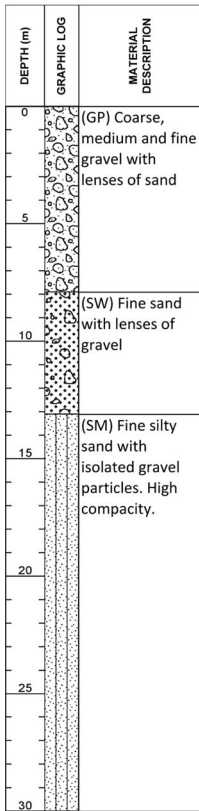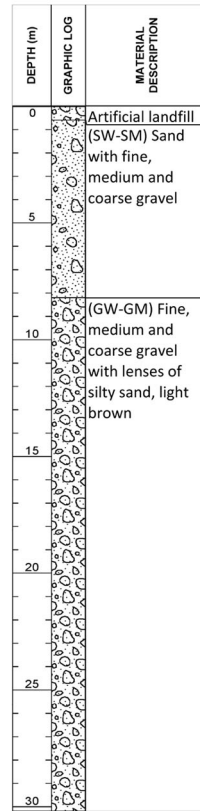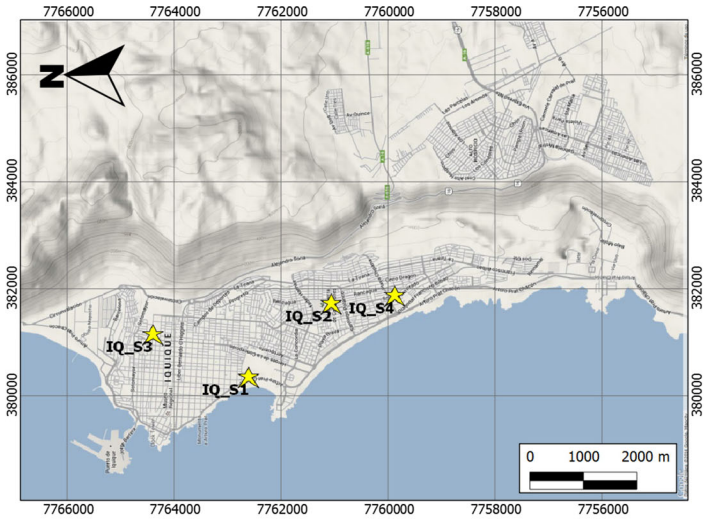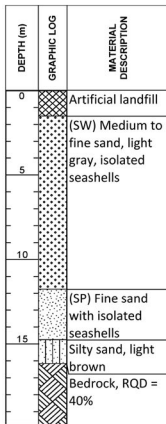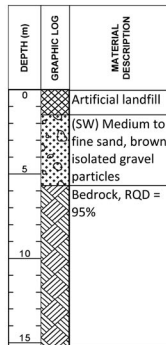
Fig. 7 **a** Location of boreholes drilled in Arica, **b–d** boreholes log
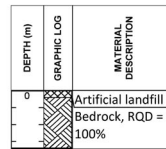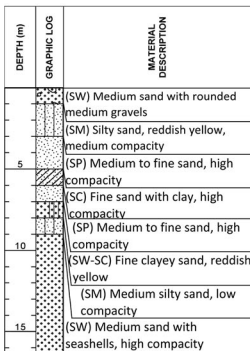
(a)

(b) IQ_S_1

(c) IQ_S_2

(d) IQ_S_3

(e) IQ_S_4

◄ **Fig. 8** **a** Location of boreholes drilled in Iquique, **b**–**e** boreholes log, where RQD denotes rock quality designation (Deere and Miller 1966)
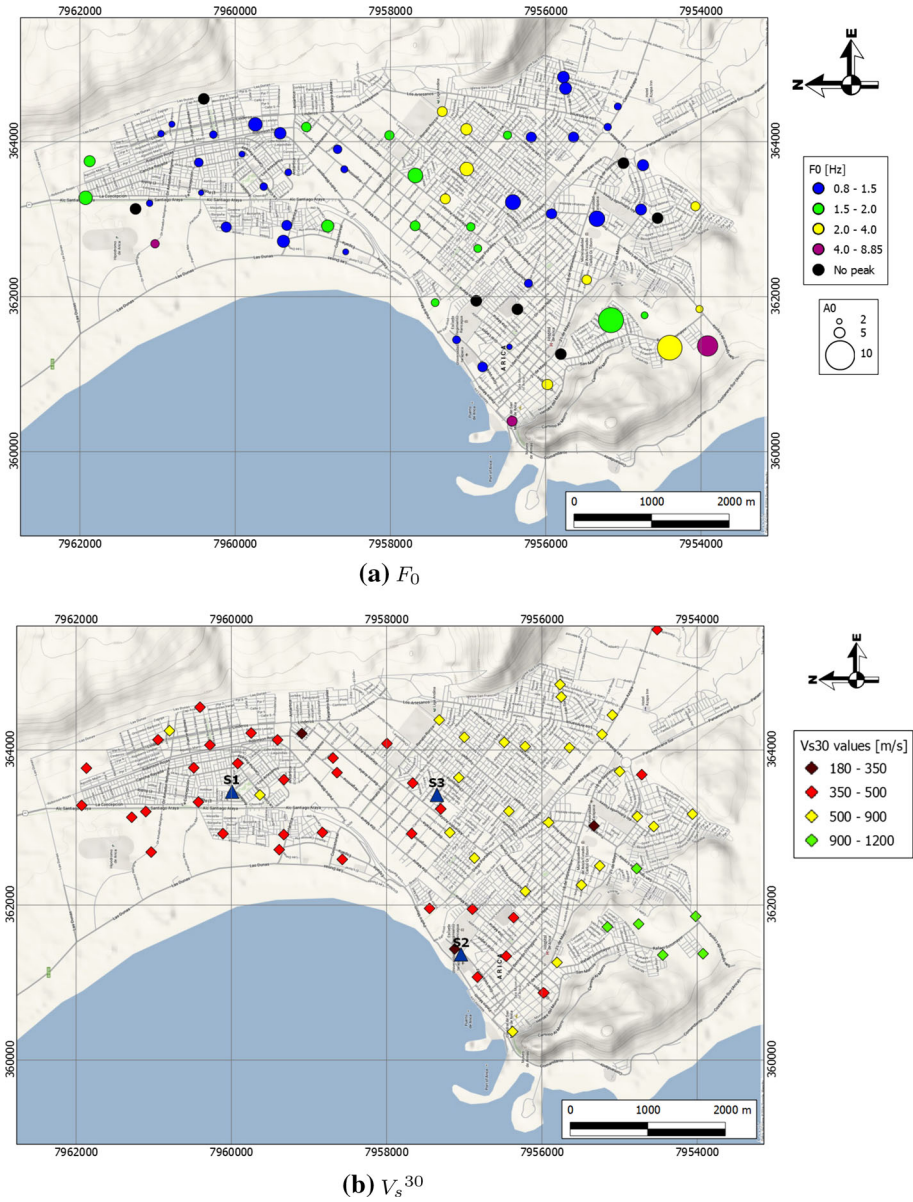

(a) F_0

(b) $V_s{}^{30}$

Fig. 9 Geophysical results in the city of Arica. **a** The values of F_0 obtained by Nakamura's technique, while **b** displays the results for V_s^{30}. *Blue triangles* denote the location of boreholes
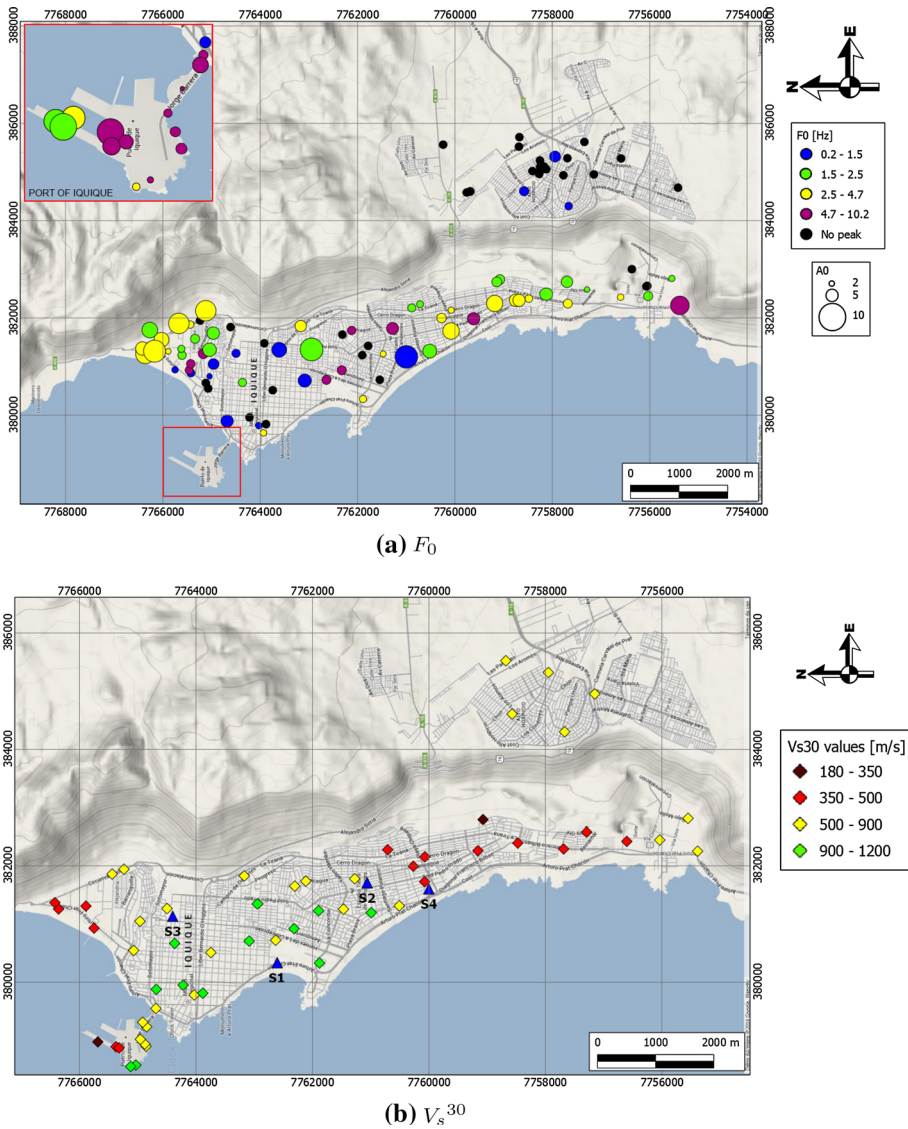
(a) F_0

(b) V_s^{30}

Fig. 10 Geophysical results in the city of Iquique. **a** The values of F_0 obtained by Nakamura's technique, while **b** displays the results for V_S^{30}. *Blue triangles* denote the location of boreholes

amplitudes of the frequencies in the south indicate the large impedance contrast between the more shallow layers and the stiffer ones of the hill. Close to the foot hills, the HV spectral ratio shows some anomalies, which are probably related to complex 3D effects of the material layers considering the mixture of limestone deposits with andesite outcrops, particularly the large green circle in the south of the city in Fig. 9a. Hence, in this area the results are not clear enough to make a robust estimation of predominant frequencies. Boreholes S2 and S3 show a mixture of rounded coarse gravel and clayey silt (Fig. 7); the samples were classified between SM and SC according to the USCS, which are a product

of the San Jose's river alluvial fan geological process. In this area, soil is stiffer than in the north, where it is mainly composed of marine deposits. Velocities are lower toward the north, as it becomes evident through borehole S1 samples, that shows the predominance of sands with almost no gravel. Tests performed in S1 samples classified the soil as a silty sand (SM) consistent with the geology maps and the geophysical surveys. There was no sign of bedrock in either the boreholes or through the shear wave velocity profile, except for the southern area, which indicated bedrock at small depths, of about 5 m.

In the northern urban limit of the city, a varied range of frequencies was found, maintaining the moderate shear wave velocities ($350 < V_S^{30} < 500$ m/s). The geological maps (Fig. 2a) identified this zone as a mixture of marine deposits with isolated deposits of diatomite. Also, velocity profiles were not able to find any sign of bedrock.
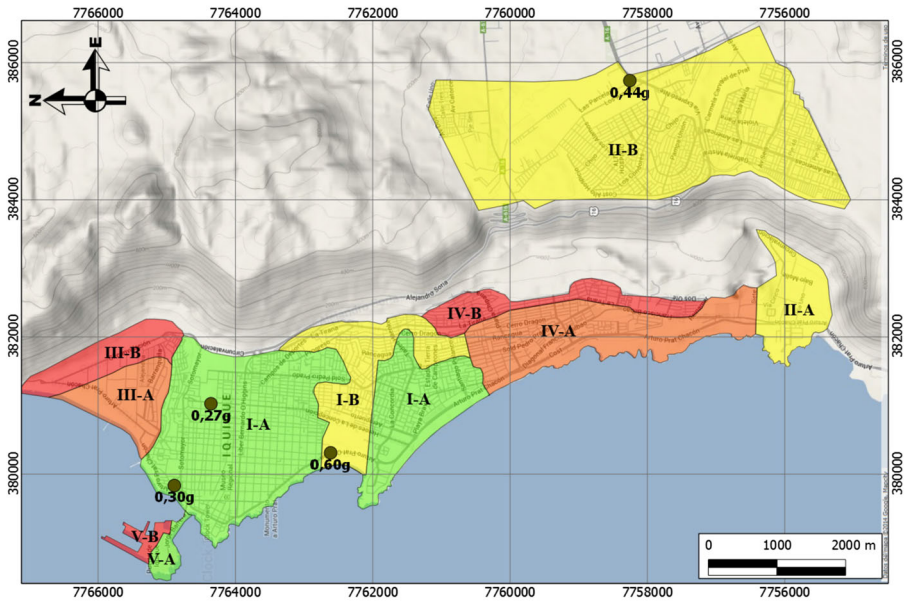
4.2 Iquique

In Iquique, the data are considerably varied; the results are displayed in Fig. 10, where velocities are fairly high in the center of the city, with a wide range of frequencies, from 0.72 to 9 Hz. This behavior may be explained by the near surface bedrock in the area. Particularly in the center of the city, some measurements showed a large H/V ratio where changes in the bedrock level are identified in the geological maps, so it is possible these anomalies are associated to shallow and thin layers of soil over the bedrock. In this particular case, the comparison between this data, the geology (Fig. 2a) and the borehole logs (Fig. 8) is highly significant. In sites where frequencies are around 2–4 Hz, the geology indicates a concentration of marine deposits, while extreme low or high frequencies (0.5–9 Hz) coincide with the presence of the bedrock outcrops. In some cases in this area, it was impossible to identify a peak on the ellipticity curves, this heterogeneous behavior of the HVSR suggests that a proper delimitation of areas based solely on geophysical information must be complemented with additional data. The boreholes are consistent with the geological background. Boreholes S2 and S3 reached bedrock at 7 and 1 m, respectively, whereas borehole S1 shows a layer of fine sand of 15 m above the bedrock (Fig. 7).

Toward the north of Iquique, predominant frequencies increase (purple circles in Fig. 10a). The very high frequency values coincide approximately with the ZOFRI Fault trace (Fig. 2c), so it is likely that bedrock's geometrical anomalies tend to affect the results of HVSR tests in this area. Velocities are relatively low ($350 < V_S^{30} < 500$ m/s), and the profiles indicate the existence of bedrock at a depth of about 20 m, which would explain the high amplitudes of the predominant frequencies in the area. To the south of the city, the velocities are the lowest ($V_S^{30} < 500$ m/s), and there seems to be a slight variation on the frequency range, decreasing from west to east, suggesting a deeper layer of soil in the eastern side. The borehole S4 is the one closest to this zone, and it shows about 15 m of sand with high compacity, mixed with varied materials (Fig. 8). Toward the southern urban limit, velocities increase and the HVSR shows high amplitudes and relative low frequencies; the velocity profiles indicate the bedrock at a depth of about 15 m.

In the area of Alto Hospicio, adjacent to Iquique to the east, the results are fairly homogeneous. Generally, large velocities are detected, but only in a few cases a predominant frequency was identified at around 1.2 Hz. Note that in the majority of the H/V computations, the spectrum is mainly plain or with low amplitudes, which is a sign of the low impedance contrast between the Alto Hospicio rigid material and the bedrock below. Hence, we can deduce that the predominant soils in this city are mainly stiff.
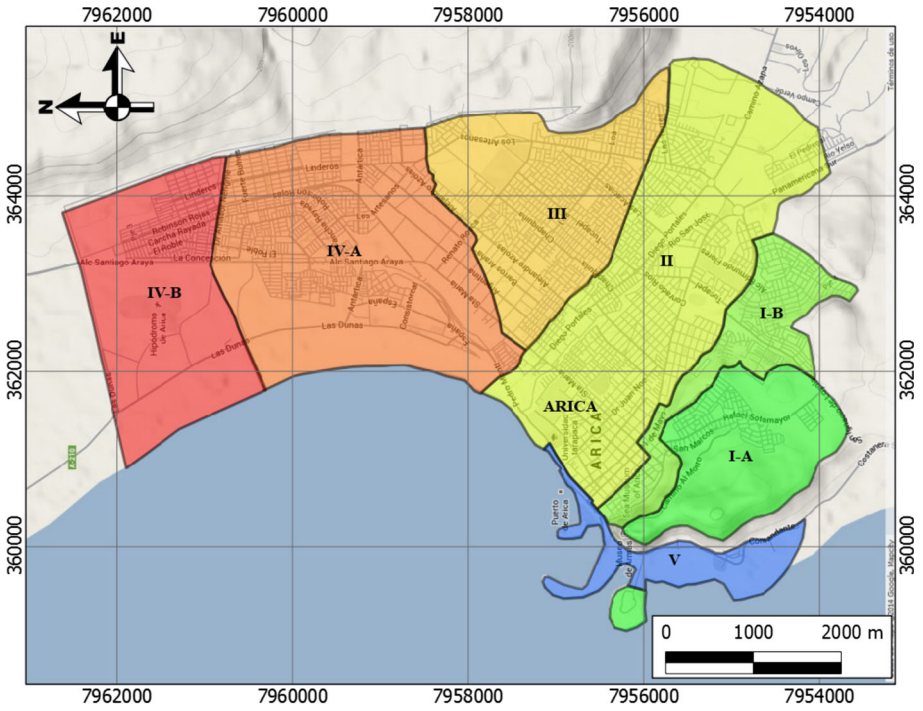
(a) Arica

(b) Iquique

◀ **Fig. 11** Proposed microzoning of **a** Arica and **b** Iquique, based on geophysical surveys, boreholes and the geological background of each area. The *colors* indicate the susceptibility of ground motion amplification in each zone, from *green* (expected low effect) to *red* (likely high effect). Additionally, the registered peak ground accelerations of the April 1 Iquique earthquake are displayed in **b**

4.3 Microzoning

The subdivision of areas was made through a joint analysis of the data obtained from geophysical surveys (shear wave velocity profiles and the HVSR), the geology maps and the boreholes. The seismic microzoning of both cities is displayed in Fig. 11, and a brief description of each zone is detailed in Table 2, which shows the average V_S^{30} and the predominant frequency range that characterizes each zone.

In Iquique, the domains where the largest ground motion amplification are expected include: the port (V-B), the north-east (III-B), and the south-east (IV-B) of the city (Fig. 11b). The zone III-B is characterized for having slightly higher V_S^{30} than to the west, because the shear wave velocity profiles detect bedrock at about 20 m deep, but the layer of sediment has a lower shear wave velocity (about 350 m/s). The HVSR amplitudes are large in this area, indicating a high impedance contrast. This zone may also be affected by topographic effects of the steep slope of the coastal range's escarpment (Fig. 2c). On the other hand, in the zone IV-B, the shear wave velocities are fairly low and the deposits appear to have a large thickness. This area may also be affected by topographic effects. Finally, the north of the port shows a thick layer of artificial landfill with low V_S^{30} (about 250 m/s). As these fillings are probably saturated, dynamic compaction or even lique-faction could take place if major events occur in this area. In areas with rigid materials or suspected bedrock outcrop, limits of predominant frequencies were not established because it was not possible to obtain a robust estimation of such parameter.
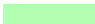
Furthermore, the peak ground accelerations of the A01-2014 Iquique earthquake, displayed in Fig. 11b, show a good correlation with the expected effects from the microzoning. The records show a minimum PGA (0.27 g) in bedrock, and the maximum PGA (0.6) g is registered where sedimentary deposits of moderate thickness were found, which indicate the effects of soft soil layers on the ground amplification. In the case of Alto Hospicio area, the recorded acceleration has a PGA of 0.44 g in agreement with the stiff soils detected in the present study.

Arica appears to have a zone with high probability of ground motion amplification toward the north, in zones IV-A and IV-B, where the lowest V_S^{30} are registered. The frequency range is fairly homogeneous and indicates a very deep layer of fine sands; in fact, shear wave profile inversions were not able to detect bedrock down to 85 m deep and borehole samples showed mostly loose sand in the first 35 m of excavation. Note that downstream San Jose's river, in the zone II, low V_S^{30} were also registered; however, the higher frequencies and the evidence of dense gravels from the boreholes suggest a lower susceptibility to ground motion amplification.

5 Discussion

The geophysical and geotechnical data acquisition and geological background of the north of Chile have provided information to properly characterize the dynamic response of the soils in the cities of Arica and Iquique at a qualitative level. This data comprise the shear

Table 2 Detailing of the zones delimited by the Fig. 11a, b

Color	Zone	Avg. V_S^{30} (m/s)	F_0 (Hz)	A0	Description
Arica					
(green)	I-A	1093	–	[2.6–9.2]	Predominance of bedrock, composed of andesite and limestone deposits
(light green)	I-B	623	[2.12–8.85]	[3.4–3.8]	Foot of the hill composed of alluvial deposits. Bedrock is located between 5 to 20 m deep
(yellow)	II	462	[0.92–1.97]	[2–5.75]	Fluvial deposits, consisting of rounded coarse gravel in a matrix of sand and silt, bedrock at deep levels
(orange)	III	530	[1.3–2.4]	[3–8.9]	Foot of el Chuño Hill, mixture of river deposits and gravels from the hill, bedrock at deep levels
(red)	IV-A	409	[0.91–1.6]	[2.1–7.55]	Marine deposits, composed of mostly fine sand. Bedrock at deep levels
(dark red)	IV-B	423	[1.07–5.43]	[2.2–6.65]	Mixture of marine deposits and diatomite, bedrock at deep levels
(blue)	V	–	–	–	Artificial landfill from the port of Arica
Iquique					
(green)	I-A	872	–	[2.05–8.55]	Andesite outcrop
(yellow)	I-B	768	[3.46–10.22]	[3.15–4.49]	Marine and eolian deposits, bedrock located at 5 to 15 m deep
(yellow)	II-A	577	[1.7–5.15]	[2.4–10]	Colluvial deposits, bedrock located at 5 to 15 m deep
(yellow)	II-B	709	–	[2.9–4.1]	Gravels from Alto Hospicio, stiff layer of gravels of about 15 m until bedrock
(orange)	III-A	461	[1.2–7.6]	[2.15–3.4]	Marine deposits, bedrock at deep levels
(red)	III-B	612	[3.25–4.1]	[2.85–8.25]	Eolian and marine deposits, bedrock located about 25 m deep
(orange)	IV-A	403	[3.03–4.68]	[2.35–6.2]	Eolian deposits of over 30 m deep
(red)	IV-B	379	[1.83–2.86]	[2.05–4.6]	Eolian and alluvial deposits from El Dragon hill, consisting mostly of fine sand, bedrock at deep levels
(green)	V-A	762	[6.84–16.85]	[2–5.9]	Andesite outcrop in the port of Iquique
(red)	V-B	393	[2.46–5.74]	[5.3–10]	Artificial landfill from the port of Iquique

wave velocity profiles and predominant frequencies of 148 sites of interest. In addition, seven boreholes were drilled to complement geophysical information and to verify the reliability of the results. A seismic microzoning, proposed before the A01-2014 event, was tested against the observation of ground motion during the earthquake. The results show the following:

1. The density of the surveys was sufficient in principle to generate a proper seismic microzoning of the soil along each city. A few exceptions are evidenced when the topography of the site or bedrock level irregularities could take a predominant role.

2. The areas in Iquique that are susceptible to site effects are; (1) the south of the city, along El Dragon hill, where a shallow layer of eolian deposits over a deep layer of sandy soil was identified; (2) to the north of the ZOFRI fault, where a marine deposit layer of approximately 15 m deep was identified; and (3) the north part of the port, consisting mainly of a thick layer of artificial landfill.

3. In the case of Arica, the main zone that is susceptible to site effects is the north of the city, where a deep layer of fine sand (over 35 m) was located.

4. Difficulties arise in the zoning definition where the transition of lithological units is suspected. Since the proposed geophysical methods assume horizontal soil layers, one must be especially cautious and consider performing local studies when there is not a robust estimation of F_0 or V_S^{30}.

5. The characterized shear wave velocity profiles reached a maximum depth of 85 m in the north of Arica using the kite-shaped arrays; this is probably enough to properly assess the ground motion amplification susceptibility, but in most of cases the information was not enough to identify a reliable depth of bedrock in most of the city.

6. The acquired data during field work are consistent with the geological context of both cities.

7. A joint analysis between F_0 and V_s^{30} is useful to assess site response; in this study, they have proven to be complementary parameters.

8. The peak ground accelerations registered for the A01-2014 Iquique earthquake agree, at a qualitative level, with the expected site effects from the proposed microzoning, further work will continue in this line considering a more exhaustive investigation regarding the earthquake.

9. The comparison between the results from geophysical tests and boreholes has shown the reliability of using surface wave-based surveys for evaluating the dynamic response of the soils.

10. Given the fact that the expected seismogenic energy accumulation of the Nazca-South American plate coupling in the north of Chile was not entirely released by the A01-2014 earthquake, the microzoning approach and results obtained in this research are a valuable tool for preventive actions within the northern Chile seismotectonic segment, which is still under high seismic risk.

References

Acerra C, Aguacil G, Anastasiadis A, Atakan K, Azzara R, Bard P-Y, Basili R, Bertrand E, Bettig B, Blarel F et al (2004) Guidelines for the implementation of the h/v spectral ratio technique on ambient vibrations measurements, processing and interpretation 169(December):1–62

Aki K (1957) Space and time spectra of stationary stochastic waves, with special reference to microtremors. Bull Earthq Res Inst 35:415–456

Astm D (2011) 2487–00 standard classification of soils for engineering purposes (unified soil classification system). Annual Book of ASTM Standards, Section 4

Bettig B, Bard P, Scherbaum F, Riepl J, Cotton F, Cornou C, Hatzfeld D (2001) Analysis of dense array noise measurements using the modified spatial auto-correlation method (SPAC): application to the grenoble area. Boll Geofis Teor Appl 42(3–4):281–304

Chavez-Garcia FJ, Cuenca J (1998) Site effects and microzonation in acapulco. Earthq Spectra 14(1):75–93

Chavez-Garcia FJ, Rodriguez M, Stephenson WR (2005) An alternative approach to the SPAC analysis of microtremors: exploiting stationarity of noise. Bull Seismol Soc Am 95(1):277–293

Chávez-García FJ, Rodríguez M, Stephenson W (2006) Subsoil structure using spac measurements along a line. Bull Seismol Soc Am 96(2):729–736

Chlieh M, Perfettini H, Tavera H, Avouac J-P, Remy D, Nocquet J-M, Rolandone F, Bondoux F, Gabalda G, Bonvalot S (2011) Interseismic coupling and seismic potential along the central andes subduction zone. J Geophys Res Solid Earth (1978–2012), 116(B12)

Comte D, Pardo M (1991) Reappraisal of great historical earthquakes in the northern Chile and southern Peru seismic gaps. Nat Hazards 4(1):23–44

Deere DU, Miller R (1966) Engineering classification and index properties for intact rock. Technical report, DTIC Document

García M, Gardeweg M, Clavero J, Hérail G, de Geología y Minería SN (2004) Hoja arica, región de tarapacá. Servicio Nacional de Geología y Minería, Santiago, Chile

Humire F, Sáez E, Leyton F and Yañez G (2015) Combining active and passive multi-channel analysis of surface waves to improve reliability of vs30 estimation using standard equipment. Bull Earthq Eng 13(5):1303–1321

Kvaerna T, Ringdahl F (1986) Stability of various fk estimation techniques. Norsar Semiannu Tech Summ 1:1–86

Lacoss R, Kelly E, Toksöz M (1969) Estimation of seismic noise structure using arrays. Geophysics 34(1):21–38

Leyton F, Ruiz S, Sepúlveda S, Contreras J, Rebolledo S, Astroza M (2013) Microtremors' hvsr and its correlation with surface geology and damage observed after the 2010 maule earthquake (Mw 8.8) at talca and curicó, central Chile. Eng Geol 161:26–33

Maldonado G (2014) Caracterización geológica de los suelos de fundación de la ciudad de Arica. XV región de Arica y Parinacota. Universidad Católica del Norte

Marquardt C, Marinovic N, Muñoz V (2008) Geología de las ciudades de iquique y alto hospicio, región de tarapacá. Carta Geol Chile Ser Geol Básica 113:33

Nakamura Y (1989) A method for dynamic characteristics estimation of subsurface using microtremor on the ground surface. Q Rep Railw Tech Inst 30:25–30

Park CB, Miller RD (2008) Roadside passive multichannel analysis of surface waves (MASW). J Environ Eng Geophys 13(1):1–11

Park CB, Miller RD, Xia J (1999) Multichannel analysis of surface waves. Geophysics 64(3):800–808

Pilz M, Parolai S, Picozzi M, Wang R, Leyton F, Campos J, Zschau J (2010) Shear wave velocity model of the santiago de Chile basin derived from ambient noise measurements: a comparison of proxies for seismic site conditions and amplification. Geophys J Int 182(1):355–367

Roma V, Tononi C (2011) Masw-remi method for seismic geotechnical site characterization: importance of higher modes of rayleigh waves. In: 12th international congress of the brazilian geophysical society

Scholz CH, Campos J (2012) The seismic coupling of subduction zones revisited. J Geophys Res Solid Earth (1978–2012) 117(B5)

Scott JB, Rasmussen T, Luke B, Taylor WJ, Wagoner J, Smith SB, Louie JN (2006) Shallow shear velocity and seismic microzonation of the urban Las Vegas, Nevada, Basin. Bull Seismol Soc Am 96(3):1068–1077

Tokimatsu K (1997) Geotechnical site characterization using surface waves. In: Proceedings of 1st international conference on earthquake geotechnical engineering, vol 3, pp 1333–1368

Tuladhar R, Yamazaki F, Warnitchai P, Saita J (2004) Seismic microzonation of the greater bangkok area using microtremor observations. Earthq Eng Struct Dyn 33(2):211–225

Wathelet M (2008) An improved neighborhood algorithm: parameter conditions and dynamic scaling. Geophys Res Lett 35(9):L09301

Wathelet M, Jongmans D, Ohrnberger M, Bonnefoy-Claudet S (2007) Array performances for ambient vibrations on a shallow structure and consequences over Vs inversion. J Seismol 12(1):1–19